Geocarto International

ISSN: (Print) (Online) Journal homepage: https://www.tandfonline.com/loi/tgei20

Investigating persistent scatterer InSAR (PSInSAR) technique efficiency for landslides mapping: a case study in Artvin dam area, in Turkey

Bulent Volkan Yazici & Esra Tunc Gormus

To cite this article: Bulent Volkan Yazici & Esra Tunc Gormus (2020): Investigating persistent scatterer InSAR (PSInSAR) technique efficiency for landslides mapping: a case study in Artvin dam area, in Turkey, Geocarto International, DOI: 10.1080/10106049.2020.1818854

To link to this article: https://doi.org/10.1080/10106049.2020.1818854

Published online: 02 Oct 2020.

GEOCARTO INTERNATIONAL
https://doi.org/10.1080/10106049.2020.1818854

Taylor & Francis
Taylor & Francis Group

Investigating persistent scatterer InSAR (PSInSAR) technique efficiency for landslides mapping: a case study in Artvin dam area, in Turkey

Bulent Volkan Yazici[a] and Esra Tunc Gormus[b]

[a]Department of Forest Engineering, Artvin Coruh University, Artvin, Turkey; [b]Department of Geomatics Engineering, Karadeniz Technical University, Trabzon, Turkey

ABSTRACT

Monitoring and determining landslides in dam reservoirs is very crucial as it is one of the main factors of dam failures in the world. Coruh river basin is one of the most important river basin in the Northeast part of Turkey which accompanies five big dams. Although persistent scatterer InSAR (PSInSAR) method is a powerful remote sensing technique which can measure and monitor displacements of the Earth's surface over time, its validation is a challenging issue because of the heterogeneous PS data. In this study, the efficiency of PSInSAR is investigated by proposing two different validation methods in order to see the consistency of the determined mean deformation velocities obtained with series of Sentinel-1A SAR-images. In the first method, 3D coordinates of reference points are projected to 1D displacement values in line of sight direction and then compared with the radar displacements of PS points. In the second method, new displacement values of PS points around reference points are identified from an interpolation map in order to be compared with the original displacements of reference points. In the end, it is showed that the displacements found by PSInSAR method are consistent with the reference points' displacements measured in the study area. Finally, this work's specific objectives are to present solutions to the challenging validation problem, to show the effectiveness of PSInSAR method and to describe the remaining challenges in PS analysis of landslide applications in dam areas.

ARTICLE HISTORY
Received 20 May 2020
Accepted 16 August 2020

KEYWORDS
Syntethic aperture radar; interferometry; persistent scatterer; PSInSAR; StaMPS; landslide

1. Introduction

Landslides in the dam reservoirs are one of the biggest threats to the dam safety. They are also one of the main causes of the dam collapses around the world. These landslides result in a large number of causalities and huge economic losses in the regions. Therefore, specifically investigating landslides around dams and their reservoirs is crucial for dam safety and future planning of the area. In order to mitigate the effects of landslides, developing early prediction and warning systems are vital importance (Scaioni et al. 2014). Landslides should be monitored and assessed regularly together with the past

CONTACT BULENT Volkan Yazici volkanyazici@live.com

activity records. In that point remote sensing (RS) is a powerful and a popular tool which collects and records earth observations by using non-contact space borne sensors. RS enables to monitor the present and the past activities over the time by using the archives of the related sensors. If one compares it with conventional systems, measuring the landslides with ground-based systems is both time consuming and very expensive. Besides, using measuring instruments can be dangerous and not practical most of the time. Because of these drawbacks, it is very advantageous to use new technologies like RS. Moreover, integrating RS sensor networks like geodetic, geological, geo-technical and environmental observations with mathematical models is a promising opportunity to develop new techniques to cope with landslides in all aspects.

Radar imaging technologies are amongst the new technologies in RS field. Using radar brings new perspectives and widens researchers understanding especially in managing natural hazards. This implies greater quantity and quality information about ground surface displacements and hence, improved landslide detection and monitoring capabilities (Wasowski and Bovenga 2014). Most of the studies of radar imaging about landslides focus on synthetic aperture radar (SAR) systems. SAR systems are active systems which use microwave lights and save the electromagnetic echoes reflected from surface to make two dimensional (2D) (amplitude and phase) complex image maps of the surface with the dimensions of slant range (sensor-target distance direction-LOS) to azimut range (satellite flight direction).

One of the most important techniques to use SAR in geological field is interferometry. Interferometry is the phase difference between two radar images, acquired at different times over the same area. The interferometric phase (Φ) is proportional to wavelength (λ) and to the difference between the two sensor-target distances (dR). dR depends on target elevation with respect to a reference surface (dR_{topo}), target displacement occured between the acquisation times of the two satellite passes(dR_{disp}), the refractivity index changes due to the presence of the atmosphere (dR_{atm}) and decorrelation sources (dR_{noise}) as seen in Equation (1) (Wasowski and Bovenga 2014)

$$\Phi = 2\pi \frac{dR}{\left(\frac{\pi}{2}\right)} - \frac{4\pi}{\lambda}\left(dR_{\text{topo}} + dR_{\text{disp}} + dR_{\text{atm}} + dR_{\text{noise}}\right) \tag{1}$$

InSAR phase data can be used to produce 3D images of Earth surface. Moreover, Differential Interferometric SAR (DInSAR) is used to detect and monitor the possible ground displacements in millimeter precision by isolating topographic contribution from the interferometric phase (Wasowski and Bovenga 2014). DinSAR has been used since 1980s (Zebker and Goldstein 1986; Gabriel et al. 1989) in measuring, mapping and detecting the possible ground surface movements (Massonnet and Feigl 1998; Singhroy et al. 1998; Costantini et al. 2000).

Traditional DinSAR which uses single pair of SAR interferormetric image has some limitations caused by incoherent changes in the target backscattering (dR_{noise}) and atmospheric disturbances (dR_{atm}). These limitations are mitigated by using persistent scatterer interferometric SAR (PSInSAR) technique which uses a set of SAR interferometry images of the same area over a long time (Ferretti et al. 2001). PSInSAR is a multi-temporal DinSAR which processes long temporal series of SAR images (usually more than 15 images) and identifies radar targets which provide a backscattered phase signal measurable through time in order to find the velocities of the ground displacements in the direction of the line of sight (LOS).

The techniques which process multi-temporal SAR images series can be grouped as PSI and Small BAseline Subset (SBAS). PSI techniques like PSInSAR (Ferretti et al. 2001)

identify persistent scatterers on interferograms which are generated by using one master image (Costantini et al. 2000; Ferretti et al. 2001; Arnaud et al. 2003; Hooper et al. 2004; Kampes 2006), whereas SBAS methods use multi-master SAR image combinations with a short temporal separation and small perpendicular baseline to reduce the effects of spatial and temporal decorrelation. They are particularly useful for processing long series of SAR imagery (Casagli et al. 2016).

There are many studies conducted to monitor volcanic, tectonic and landslide activities by using PSInSAR technique. Very extended research is presented by Farina et al. (2006) specifically about determining landslides by using PSInSAR method. In the work by Farina et al. (2006), ERS-1 and ERS-2 SAR images were used to help the landslide inventory mapping in Arno river basin (Italy). In the end, it is declared that existing landslides were re-identified clearly as well as new unstable areas by using PSInSAR technique.

In another study done by Meisina et al. (2006), PSInSAR technique is used for detecting and monitoring ground displacements in the Oltrepo Pavese territory (Northern Italy). In their study, the state of activity of several landslides was revised and some previously unknown unstable slopes were detected in areas with shallow and deep landslides. With PSInSAR technique, slow ground deformations were detected between 5 and −16 mm/year at a sub-regional scale. In the work by Ciampalini et al. (2016), a new technique was developed by using PSInSAR to increase the accuracy of the susceptibility map which is very important in land use and planning activities. PSInSAR data were combined with susceptibility map to improve the prediction reliability of slow moving landslides, which particularly affect urbanized areas. Mateos et al. (2017) integrated PSInSAR data with geological and hydrogeological information for better understanding of subsidence process in Vega de Granada. SAR data, obtained from ENVISAT, Cosmo-Skymed and Sentinel 1A, were used for monitoring ground motion. Authors have found good correlation between groundwater level depletion and rapid ground water response. Bayer et al. (2018) also used Sentinel 1A images together with Cosmo-Skeymed images to monitor slow moving landslides and investigate responses of landslides according to different geological structures in Northern Apennines of Italy. Authors have monitored spatial displacement between 2009 and 2016 for 25 landslides in the region successfully.

As so many authors have used PSInSAR method for monitoring and mapping landslides, not too many of them have studied the validation of this technique. In the work by Ferretti et al. (2001), the efficiency of PS technique on ERS DInSAR data has been validated with the displacements found by GPS and optical levelling methods. Authors have found high correlation between PS and other methods (GPS and levelling) by exploiting >55 ERS images, which dates from 1992 to 2000. Levelling and GPS displacement values have been projected to LOS direction and compared with the time series of the nearest PS point. For levelling the agreement has been interpreted visually and 5–10 mm of vertical accuracy has been found for GPS points within 100 m away from PS on the Italian coast South-West of Ancona with a slow evolving landslide. In another study (Ferretti et al. 2007), artificial reflectors, which are objects that exhibits a high radar cross-section stablity in time, have been exploited together with GPS data to assess the accuracy of the InSAR measurements. In the experimental setup carried out in the study, reflectors have been mounted in order to be visible in both Envisat and Radarsat acquisition. The ground truth has been compared with the InSAR data by moving one pair of dihedral reflectors a few millimetres between SAR acquisitions, in the vertical and east–west (EW) directions. In another comprehensive study (Notti et al. 2014), a methodology has been proposed to improve the PSI data analysis for landslides. To do an accurate evaluation and validation, five different SAR data sets have been processed with three different PSI techniques. The

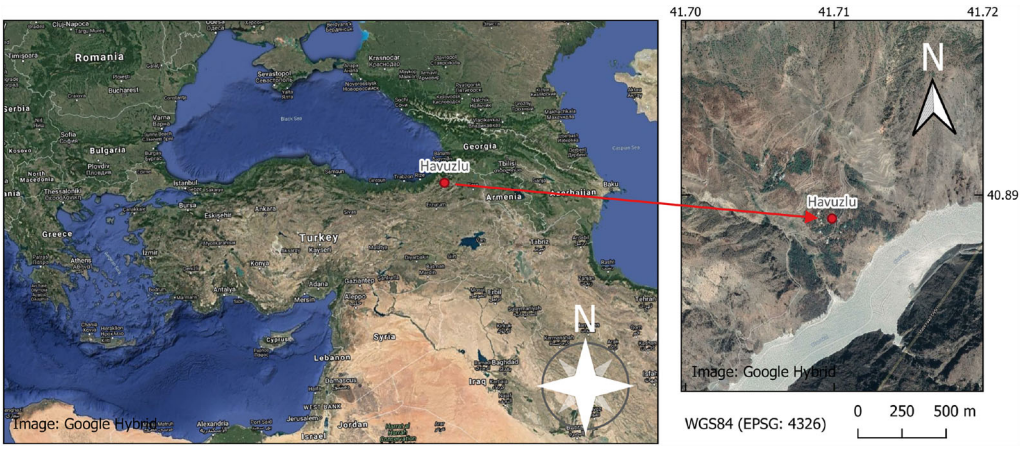

Figure 1. Geographical location of the study area.

validation part has been carried out by transferring the raw PS data into the best information by defining the threshold of activity, projecting the LOS velocity along the slope, estimating the EW and vertical velocity components and identifying the anomalous area.

In this study, PSInSAR technique is carried out with 25 Sentinel images on one side of a hill with a slow evolving landslide. Then, the efficiency of PSInSAR is investigated by proposing two validation methods. Furthermore, as stated by Köthur et al. (2016), PSI method is a difficult technique to apply. Apart from the processing steps, the validation of its results is also challenging. Ideally, the PS data must be compared with geodesic methods like levelling and GNSS ground truth (Colesanti et al. 2001). However, what makes this difficult is twofolds. First, the heterogeneously scattered PS points may not be overlapped with the reference data to compare the displacement of that point and the second is, the coordinates and acquisition dates of ground truth and PS data that usually may not match. Therefore, this study aims three different targets. First, one is to show the effectiveness of PSInSAR method on the identification and monitoring of slow-moving landslides in the dam reservoirs by using Sentinel 1A data. The second one is, to present solutions to one of the challenges of PSInSAR applications of how to match the heterogeneous PS data with the reference data during validation and third one is, to describe the remaining challenges in PS analysis to the earth-science communities.

After giving introduction in the first section, rest of this article is written as follows: The study area is described in Section 2. The data set used in PSInSAR method, the technique itself and the proposed validation framework are given in Section 3. Implementation and validation results of PSInSAR method are given in Section 4. Discussions are given in Section 5 and finally, conclusions are drawn in Section 6.

2. Study area

The Çoruh River in Artvin (NE of Turkey) is one of the most important rivers of Turkey with five dams and many hydroelectric power systems on it. Because of its topographical structures and extensive construction in the area, the river basin is very prone to the landslides. Landslides formed on the valley slopes of dam reservoir sites are very dangerous both for the dam itself and for the people in the area. For these reasons this study is conducted on an existing landslide area in Havuzlu village called Havuzlu paleo-landslide which is in the Artvin Dam reservoir area on the Çoruh river basin (Figure 1). The

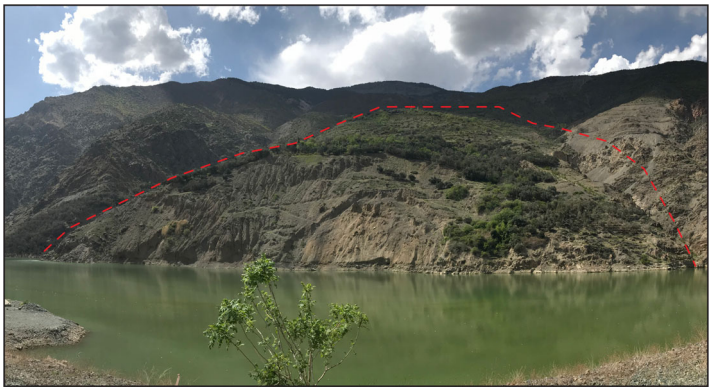

Figure 2. Side view of Havuzlu region.

borders of the landslide are also presented on a satellite image in Figure 2. Havuzlu Village is expropriated and then evacuated because of the frequent landslides activities in this area. After evacuation, the ground motion was monitored by conventional measuring methods but not with RS methods like PSInSAR technique.

3. Methodology

The methodology exploited in this research is described under the following two subsections. First, the PSI method and the image set used for this technique are explained together with the processing steps. Then, the proposed validation framework is introduced.

3.1. PSI method

After radar-based measuring systems become popular in geological applications, new techniques like PSInSAR were introduced to the community by the researchers. As stated earlier, PSInSAR uses multi-temporal interferometric images that help to overcome some of the limitations of conventional DinSAR method. Therefore, it is successfully used in landslide investigation applications. In this article, PSInSAR is used to investigate the landslides in the dam reservoir areas.

The work flow followed in this study is presented in Figure 3 and divided into four blocks. According to Figure 3, in the first block, Sentinel 1A, C band, SAR image data are gathered in the required time range. A master image is selected amongst these data sets and pre-processing step is started as the second step. In the second block, Sentinel application platform (SNAP) which is a Sentinel image processing toolbox is used to do orbit correction, geographical coding and interferometry. Then, final product is transferred to StaMPS/MTI (Stanford Method for Persistent Scatterers/Temporal InSAR) to generate persistent scatterer (PS) points. So, the third block is conducted in StaMPS. In StamPS, these steps are followed respectively; data are loaded, phase noise is estimated, PS points are selected, unrelated PS points are cleared, phase wrapping is done, spatially correlated look angle (SCLA) error is estimated and atmospheric filtering is applied. Finally, in the fourth block, the output data are edited and analyzed to be visualized. When the analyses are done, user has LOS displacement time series, mean LOS displacements and refined elevation estimates of each PS point in the area. At the end of analysis, displacements in

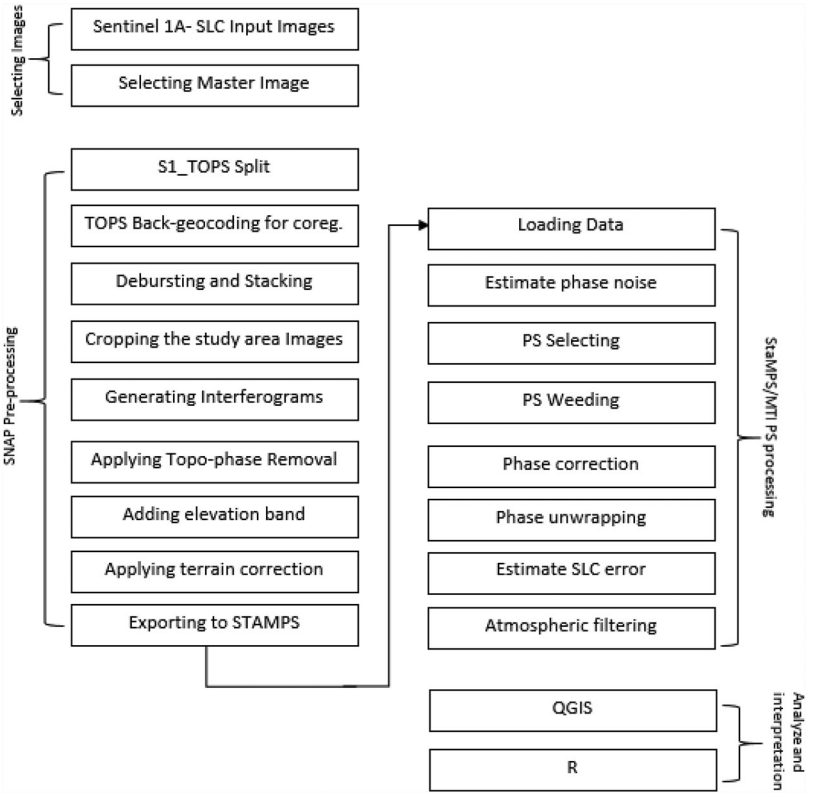

Figure 3. Workflow diagram of PSInSAR method followed in this study.

LOS direction are compared with field measurements, to investigate the consistency of the PSInSAR technique.

In order to apply the PSInSAR technique, series of SAR images are needed to be obtained in the related time range. SAR images can be obtained from different platforms both public and private. In this study, SAR images belonging to Sentinel 1A are used and downloaded from Copernicus Open Access Hub (Copernicus 2018) and Alaska Satelite Facility's (ASF) portal called Vertex (Vertex 2018). Detailed information and dates about the images used in this study are listed in Table 1. StaMPS/MTI software (Hooper et al. 2012) which uses Stanford PSInSAR method and works on both Matlab and Linux OS is used to generate PS points. The blocks mentioned in the pre-processing section in the workflow can be done by using toolboxes like The InSAR Scientific Computing Environment (ISCE), SNAP and GAMMA. In this study, SNAP is used as it is developed specifically for Sentinel images. The output results generated at the end of the last section of workflow are visualized in QGIS and R programs for further analysis.

3.1.1. Image selection and processing steps

When the images are downloaded with the same frame number among images with the same flight direction (ascending or descending) over the study area, an image is selected as a master image and others are grouped as slave images. The temporal base length should be considered while choosing the master image. The acquisition date of the master image should be in equal distance to the acquisition dates of the other slave images as

Table 1. List of images used in this study.

Date	Sensor	Frame (Track)	Orbit	Btemp (Day)
3 January 2018	S-1A	145	19,992	180
15 January 2018	S-1A	145	20,167	168
8 February 2018	S-1A	145	20,517	144
20 February 2018	S-1A	145	20,692	132
4 March 2018	S-1A	145	20,867	120
28 March 2018	S-1A	145	21,217	96
9 April 2018	S-1A	145	21,392	84
21 April 2018	S-1A	145	21,567	72
3 May 2018	S-1A	145	21,742	60
15 May 2018	S-1A	145	21,917	48
8 June 2018	S-1A	145	22,267	24
20 June 2018	S-1A	145	22,442	12
2 July 2018[a]	S-1A	145	22,617	0
14 July 2018	S-1A	145	22,792	−12
7 August 2018	S-1A	145	23,142	−36
19 August 2018	S-1A	145	23,317	−48
12 September 2018	S-1A	145	23,667	−72
24 September 2018	S-1A	145	23,842	−84
6 October 2018	S-1A	145	24,017	−96
25 October 2018	S-1A	145	24,862	−156
30 October 2018	S-1A	145	24,367	−120
11 November 2018	S-1A	145	24,542	−132
23 November 2018	S-1A	145	24,717	−144
17 December 2018	S-1A	145	25,067	−168

[a]Master image.

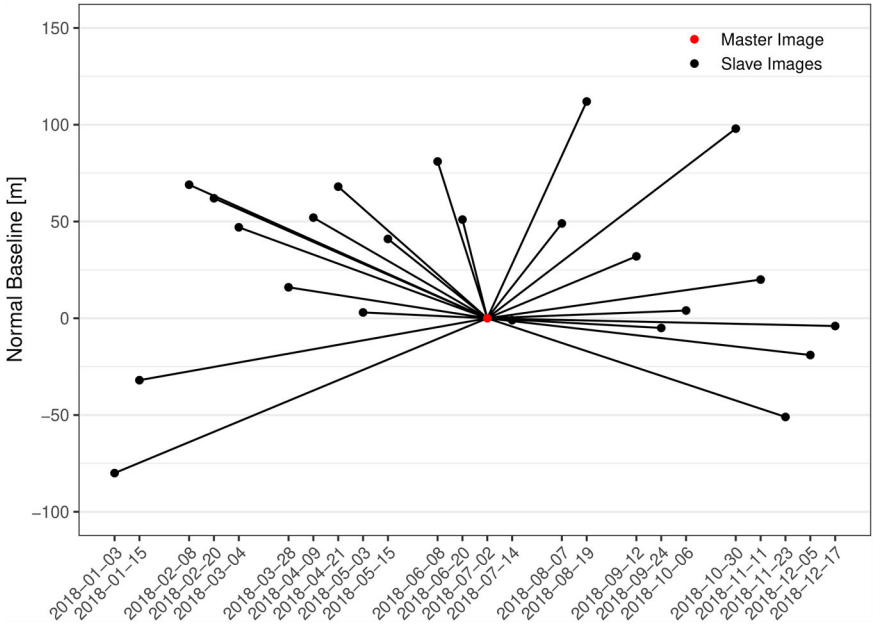

Figure 4. Star graph of the SAR images used for Havuzlu village.

shown in Figure 4. When images are ordered chronologically, the master image is chosen to be the one in the middle. Here, temporal base length is considered as the main criteria.

In PSInSAR technique, different types of graphics are used to analyze the temporal distance of master and slave images during generation of interferograms. Graphic types like MST, Full Graph, Small Temporal Baselines are used with SBAS and Quasi-Permanent

Table 2. Important parameters used during SNAP and STAMPS/MTI processing.

Software	Parametre	Havuzlu
SNAP	Back-Geocoding and Interferogram Formation	SRTM 3 Sec
SNAP	Back-Geocoding – DEM Resampling Method	Bilinear interpolation
SNAP	Back-Geocoding – Resampling Type	Bilinear interpolation
SNAP	Interferogram Formation – Subtract Flat Earth Phase	used
SNAP	Interferogram Formation – Degree of Flat Earth Polynomial	5
SNAP	Interferogram Formation – Orbit Interpolation Degree	3
SNAP	Interferogram Formation – Subtract Topographic Phase	Used
StaMPS/MTI	filter grid size	15
StaMPS/MTI	scla deramp	y
StaMPS/MTI	unwrap method	3D
StaMPS/MTI	unwrap grid size	200
StaMPS/MTI	unwrap gold n win	32
StaMPS/MTI	unwrap gold α	0.8
StaMPS/MTI	ref centre lonlat	41.716260, 40.885728
StaMPS/MTI	ref radius	20
StaMPS/MTI	ref point	1

Scatterers (QPS) methods, whereas Star Graph is used in Stanford method. The star graph of image series used in our study is shown in Figure 4.

After selecting the master image in SNAP, crop the study area for quick and easy image processing in the computer with the help of TopSAR Split operator. Sentinel-1 TOPSAR Split operator is applied to both master and slave images to get the same sub-swath and the same polarization data from selected bursts for co-registration. Then, apply precise Orbit File to correct the orbits. Orbit File provides accurate satellite position and velocity information to all images. After this, co-registration is completed with back Geocoding operation. This operator co-registers master and slave product using orbits of the product and a Digital Elevation Model (DEM). During this process Thermal Emission and Reflection Radiometer (ASTER), or Shuttle Radar Topography Mission (SRTM) type of DEM can be used and can be provided by the software or by the user. For DEM resampling, methods like nearest neighbour, bi-linear, bi-cubic etc. can be used in SNAP. Master image must be the first image during these processes.

In de-bursting and merging steps, the bursts are concatenated and sub-swaths are merged to form one image. You do this step if your study area is covered by more than one burst. Bursts overlap minimally in azimuth and sub-swaths overlap minimally in range. Bursts for all beams have been resampled to a common grid during azimuth post-processing. In the range direction, for each line in all sub-swaths with the same time tag, adjacent sub-swaths are merged. For the overlapping region in range, merging is done midway between subswaths. In the azimuth direction, bursts are merged according to their zero Doppler time. The output of this operator is the deburst product (Hooper et al. 2010). New image is formed with one side in the length of subswath and other side in the length of the used burst. The study area is cropped from this image with the help of sub-set operator. After cropping the working area from the image, interferograms are computed. At the end of pre-processing step, interferograms are transferred to StaMPS/MTI software in order to be used to generate PS points (Comut 2016). After pre-processing steps, PS generation is started in StaMPS/MTI software and followed the steps presented as in Figure 3. Briefly, StaMPS/MTI software exploits Matlab in Linux and uses command line to do the PS processing. First, load data and store in Matlab work space. Second, estimate phase noise value for each candidate pixel in every interferogram. Here user decides the iteration number. Third, pixels are selected on the basis of their noise characteristics in the PS selection. Then, these pixels are kept or dropped according to their signal contribution or noise level. The wrapped phase of the selected pixels is corrected for spatially

Figure 5. Reference points used in the field H-1, H-2, DEF-2 and DEF-13 respectively from left to right.

uncorrelated look angle error in the fifth step. This step is followed by Phase Unwrapping step. Finally, PS processing ends by estimating the SCLA error which is due to incorrect mapping of the DEM into radar coordinates. Atmospheric filtering step is carried out optionally. But, it is carried out in this study as it improves the unwrapping accuracy. After executing three blocks, now user has PS points with their displacements in a text file (Hooper et al. 2010). In the fourth block, in Figure 3, PS points in text file are transferred to QGIS for generating result figures. All the figures (except time series) are drawn in QGIS. The 'ggplot' tool in R is also used in this study to draw the 'Time Series' figures. Important parameters that are used in this study for PSInSAR method are listed in Table 2.

3.2. Proposed validation framework

To investigate the landslide in Havuzlu, a private company has done continuous measurements with electronic distance measurement (EDM) instruments called Leica TS-06. They have built a small network with two reference points (H1 and H2) and 10 reference points (DEF-1, DEF-2, etc.). They have used H-1 and H-2 as a starting point on a stable area and then measured other 10 reference points three times, and the average of these measurements has been set as final coordinates. Then the displacements of these points are calculated simply by taking the difference of coordinates. Figure 5 shows pictures of H1, H2, DEF-2 and DEF-13 points in the field with reflectors built on them. An overview of the mentioned network is also presented in Figure 8.

Both the PS points and the measured points are demonstrated in Figure 8. Although there are not any PS points exactly on the measured points (DEF points) for comparison reasons, there are still plenty of PS points placed very close to the DEF points.

In this stage of the study, two different methods are used in order to measure the consistency of the PSInSAR results. These methods are explained briefly in the following subsections.

3.2.1. Comparing 1D in situ observations with PS LOS displacements

In the first validation method, 3D coordinates of DEF reference points are obtained from in situ observations which are taken as reference data.Their 3D coordinates are projected to 1D displacement values in LOS direction and then compared with the radar LOS displacement of PS points. PS points around DEF-2 and DEF-13 are selected according to a

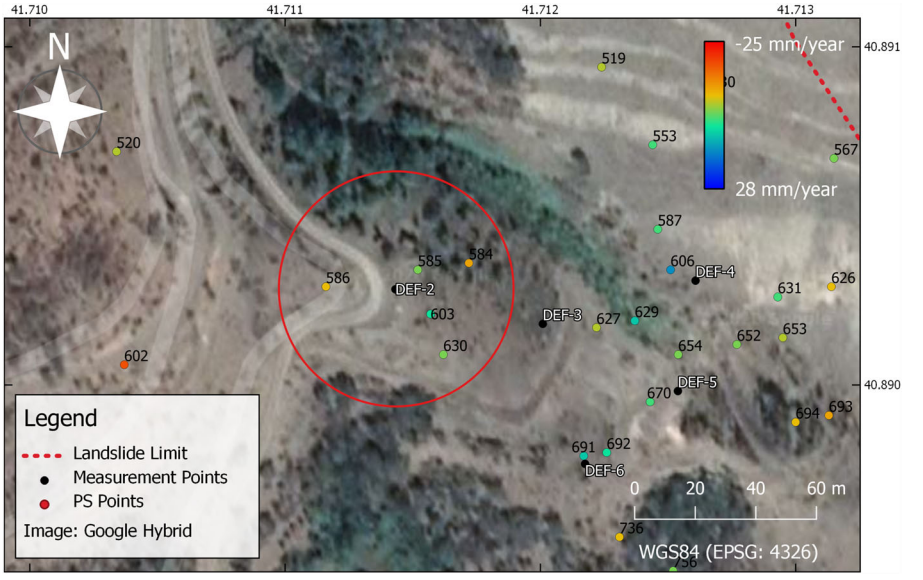

Figure 6. Reference point DEF-2 and PS points around it.

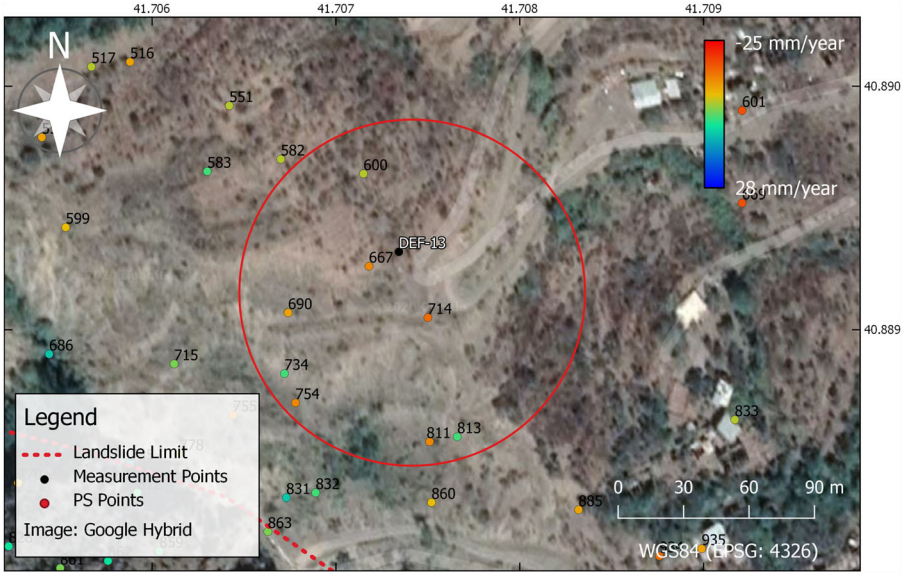

Figure 7. Reference point DEF-13 and PS points around it.

radius around the point as none of them exactly overlapped in the field. These PS points are shown in Figures 6 and 7, respectively.

Using the 3D displacement vectors obtained from in situ observations, the radar LOS displacement can be computed through a simple forward model. Let the surface displacement orthogonal components be $D = (dx, dy, dz)$, in east, north and vertical (up) directions, respectively, for a given point at the Earth's surface. Then, the projection of the surface displacement vector D to the line of sight can be formulated as in Equations (2) and (3):

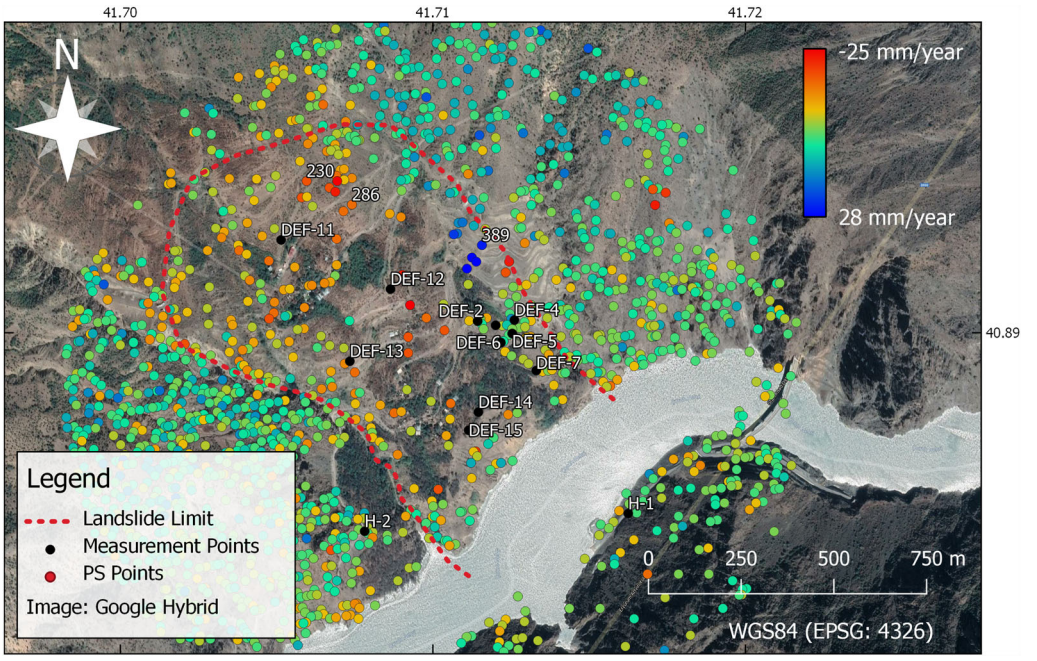

Figure 8. This figure includes: PS points in and around the landslide with displacement values in different colours, and reference points measured by terrestrial methods (with DEF prefixes).

$$d_{\mathrm{LOS}} = \hat{s} \cdot D \tag{2}$$

$$\hat{s} = \begin{pmatrix} -\cos\alpha_{\mathrm{h}} \sin\theta_{\mathrm{inc}} & \sin\alpha_{\mathrm{h}} \sin\theta_{\mathrm{inc}} & \cos\theta_{\mathrm{inc}} \end{pmatrix}^{T} \tag{3}$$

d_{LOS}, $\hat{s}$, θ_{inc} and α_h denote line-of-sight displacement, the satellite unit vector, the radar incidence angle at the scattering point and the azimuth heading of the satellite, respectively (Arikan and Hanssen 2008). Incidence angle and the azimuth heading values were obtained from the master image in order to calculate the LOS. It is important to remember that positive LOS magnitude values show surface uplifts and negative LOS shows subsidence relative to the chosen master image.

The satellite LOS is roughly nine and four times more sensitive to vertical displacements and the displacements in x (east) direction, respectively, compared to the component in the y (north) direction. This is due to the near-polar satellite orbits and the incidence angle of $\theta \cong 23^{\circ}$ (Arikan and Hanssen 2008).

The results of this comparison are given in Table 3 and these will be discussed in Section 4.

3.2.2. Comparing in-situ observations with interpolated PS LOS displacements

In the first validation method, displacements of PS points generated by PSI method and reference points measured by traditional geodetic methods were compared. In this subsection, second validation method will be presented. In this method, in order to validate the displacement of the PS points, an interpolation map is created as shown in Figure 11 and the reference (DEF) point's 1-D displacements are compared with the new velocity values obtained from this map.

Interpolation map is created by using Kriging (ordinary) method. Kriging is chosen as its performance in generating digital elevation model (DEM) with SRTM data is better compared to other contemporary methods like Inverse Distance Weighted, ANUDEM,

Table 3. Comparison of the displacements of DEF-2 and DEF-13 reference points with the closest PS points around them in LOS direction in one year.

Ref. point	Displacement (mm/year)	Distance between DEF and PS (m)	PS points no.	Displacement (LOS) (mm/year)
DEF-2	−0.43	25.74	584	−11.41
		9.78	585	−2.77
		22.96	586	−6.28
		14.12	603	0.48
		26.58	630	−6.10
			Mean disp:	−5.21
DEF-13	−1.84	39.13	600	−5.14
		15.21	667	−14.96
		57.85	690	7.44
		32.72	714	−12.43
		76.35	734	−7.62
		85.55	754	−16.26
		87.69	811	−10.50
		88.47	813	6.30
			Mean disp:	−6.65

Nearest Neighbour and Spline (Arun 2013). Kriging method is an interpolation method that uses the weights of the surrounding points in order to estimate the the value of the unknown points. The equations of Kriging methods are given in Equation (4) (Tural 2011). The results of this method will be given in Section 4

$$N_{\mathrm{p}} = \sum_{i=1}^{n} P_i \times N_i \tag{4}$$

In this equation (N_{p}) is the unknown points value, (n) is the number of points that generates the model, (P_i) is the weight value, (N_i) is the point's measured value (Yaprak and Arslan 2008).

4. Results

A picture of the landslide area in Havuzlu, Artvin is given in Figure 2. PSInSAR technique is applied on Havuzlu landslide by using 24 Sentinel 1-A SAR C band, SLC images with ascending orbit and in VV polarization as shown in Table 1. The SAR image taken on 2 July 2018 is selected as master image. In this section, the results of PSInSAR technique and the results of validation method will be given, respectively.

4.1. PSI results

Displacement velocity of the PS points is shown in Figure 8. In this figure, ground displacements in LOS direction are found between −25 mm and +28 mm. The points with highest velocity are placed around the border of the landslide where the unstable area starts in dam reservoir. This shows that PSInSAR method is successful in detecting the existing landslides. In fact, there are less PS points in the landslide area than the surrounding.

In Figure 9, the displacements of PS point numbers 230 and 286 were found as −22.01 and −5.99 mm/year respectively. The direction of displacement in both points is negative which means the distance between points and the sensor was increased in the LOS direction. Whereas, in Figure 9 where the displacement of PS number 389 was found +24.02 mm/year, the distance between point and the sensor was decreased in the LOS

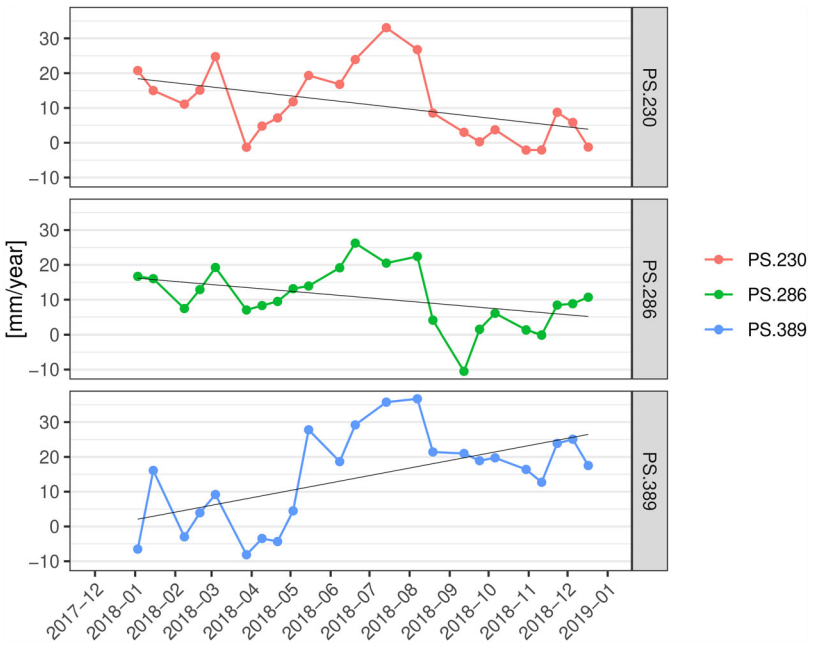

Figure 9. Time series analysis of PS point number of 230, 286 and 389 in Havuzlu.

direction. It can be concluded that, PS points with positive velocities indicate surface deformation motion upward and eastward, while negative deformation rates reflect movements downward and westward (Tofani et al. 2013).

In total, 1688 PS points were created in the area after the PSInSAR processing. In Figure 8, PS points with 230, 286 and 389 were chosen to show their displacements over the time series graphics in Figure 9.

4.2. Validation results

The results of first validation method are presented in Figure 10 and Table 3. Figure 10 and Table 3 show the comparison of the displacements of DEF-12 and DEF-13 with the PS points around them in LOS direction. In Table 3, the maximum difference was obtained between DEF-13 and PS 754 as 14.42 mm, where they are 85.55 m apart from each other.

In the second validation method, an area is selected where the PS points are intense and close to the DEF reference points in the first step. In this area there are reference points named DEF-2, DEF-3, DEF-4, DEF-5, DEF-6 and PS points numbered as 584–585–587–603–606–627–629–630–652–654–670–691–692–736. 1D displacements of the reference points (DEFs) are calculated by using Equations (2) and (3) in the LOS direction to be able to be compared with the PS points. That was presented in Table 4. Then Kriging interpolation is applied by using the 1D displacements in the LOS direction of 14 PS points. Then, new displacements values overlap with DEF points are obtained from this map. Finally, the displacements of DEF points which are obtained by two different methods (one from the coordinates of the DEF points measured in the field and the other from the weights of PS points) are compared with each other.

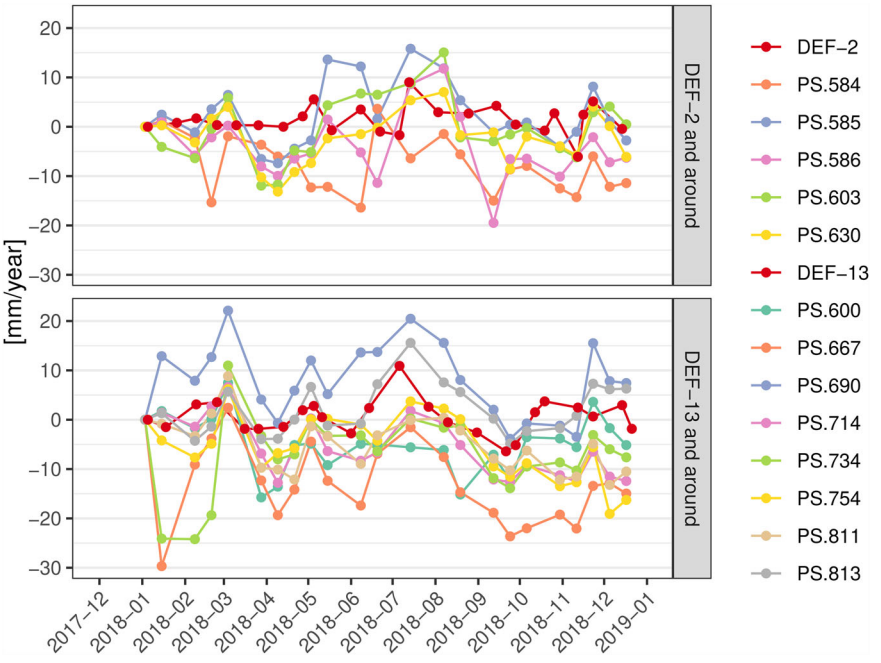

Figure 10. Comparison of monthly displacements of DEF-2 and DEF-13 reference points with PS points around them.

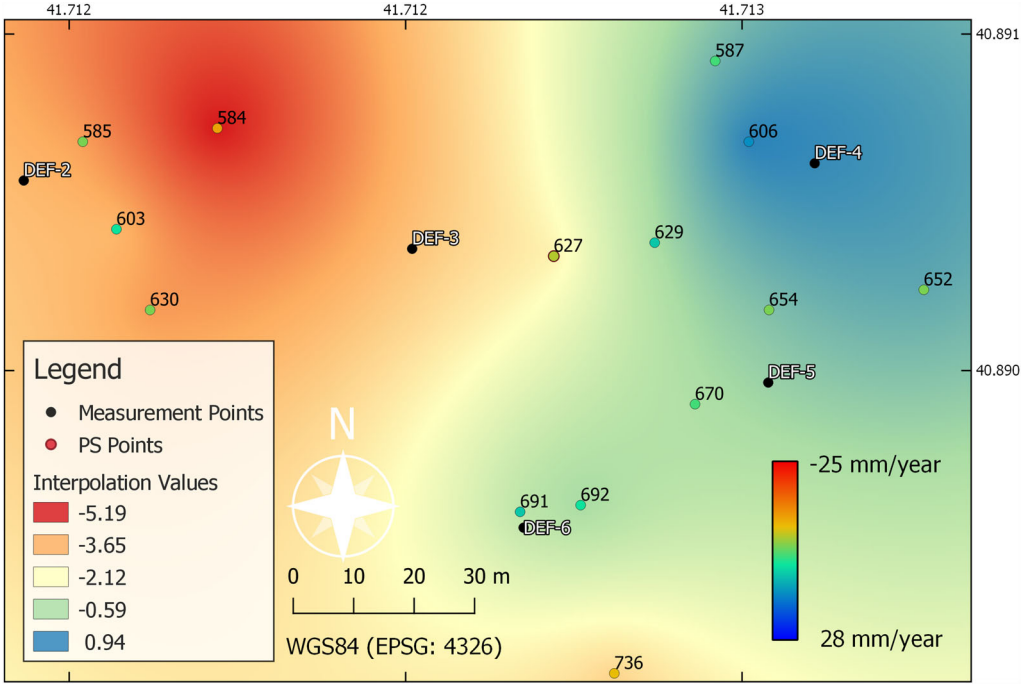

Figure 11. Interpolation map that is created by using the displacements of PS points in LOS direction around DEF-2, DEF-3, DEF-4, DEF-5 and DEF-6 reference points.

Table 4. Comparing the 1D LOS displacement values of original reference points (DEFs) generated from the coordinates measured in the field and new values of reference points that are generated from the weights of PS points by an interpolation methods.

Points	Original LOS displacements (mm/year)	New LOS displacements (mm/year)	Differences (mm/year)
DEF-2	−0.43	−3.45	3.02
DEF-3	−2.40	−3.23	0.83
DEF-4	2.75	0.81	1.94
DEF-5	−0.27	−0.37	0.10
DEF-6	−2.18	−1.04	−1.14

5. Discussion

In this study, PSInSAR method is employed to monitor the existing landslides and to find new unstable areas in the dam reservoir in Havuzlu village in Artvin/Turkey. At the end of our study, the total displacements of PS points in Havuzlu are found between −25 and +28 mm/year in LOS direction by using PSInSAR method. In order to investigate the validation of InSAR, DInSAR and PSInSAR techniques, genarally GPS ground control points are used in most of the studies (Vilardo et al. 2009; Tamburini et al. 2010; Zhang et al. 2012; Lagios et al. 2013). In this study, GPS points are not available, so reference points measured by EDM are used in Havuzlu study area. Field work has been carried out between 03 January 2018 and 17 December 2018. Therefore Sentinel 1A images were downloaded in these time intervals.

In our study, reference points named DEF-2 and DEF-13 and PS points around them are used as they are presented in Figures 6 and 7, respectively. Table 3 gives the final displacements of two DEF points and closest PS point around them including their distances to DEF points. In this table, the LOS displacement of DEF-2 and the nearest PS point around it (∼9.8 m) are found −0.43 mm/year and −2.77 mm/year, respectively. Total mean displacement of five PS points (numbered as 584, 585, 586, 603 and 630) in the neighbourhood of DEF-2 is found −5.21 mm/year. On the other hand, the displacement in LOS direction of DEF-13 and the nearest PS point around it are found −1.84 mm/year and −14.96 mm/year, respectively. Total mean displacement of eight PS points (numbered as 600, 667, 690, 714, 734, 754, 811 and 813) around DEF-13 is found to be −6.65 mm/year. As a result, in Table 3 it is presented that the difference between the displacement values of PS values and reference points are in mm scale.

Validation results are also presented on graphics for better understanding and comparison. Two validation process are carried out in this study to present the effectiveness of PSInSAR technique in detecting and monitoring slow-moving landslides in the dam reservoir areas. In the first validation process, 1D displacements of DEF-2 and DEF-13 points are compared to displacements of PS points through out a year in time series graphic in Figure 10. By taking into account the fact that none of the PS points are exactly overlapped with the reference points, and reference points are compared with the closest PS points, it is found that the trends of the displacements of PS points are correlated with the references in the field. This shows that PSInSAR method is capable of tracking the displacements of points in the field by using remotely sensed images.

In the second validation process, 1D displacements of reference points in Havuzlu area are calculated by using Equations (2) and (3). Then, an interpolation map is created with the displacements of 14 PS points around DEF points by exploiting Kriging interpolation method. Finally, new displacement values in LOS direction for DEF points are identified from interpolation map. Both the calculated displacements and interpolated displacements of DEF points are presented in Table 4.

When we compare the differences of displacements for DEF points, maximum difference is found as 3.02 mm/year for DEF-2 and minimum displacement is found as 0.10 mm/year for DEF-5. Besides, according to the yearly displacement values in Table 4, one can see that the direction of the interpolated displacements of all five DEF points is the same with the calculated ones. In another word, both displacements are in the same direction which shows the displacements of PS points generated with PSInSAR method are consistent with the reference points in the field. In the end, it can be concluded that the displacement values found by PSInSAR method are reliable for further process and decision making authorities.

Overall, the accuracy of PSI technique, hence the displacement differences between DEF and PS points, depends on different criteria like number of images, using both direction modes (ascending and descending), vegetation on the area, resolution of the images (high-resolution X-band data (TerraSAR-X, Cosmo-SkyMed)), topography and the type of point used as a reference. Using GPS, levelling (Colesanti et al. 2001) or reflector points (Ferretti et al. 2007) and higher resolution SAR images more than 25 would increase the PSI accuracy and decrease the displacement differences between DEF and PS points. But, when these conditions are not available, terrestrial instrumental measurements are used like in this study. In this situation, landslide activity can be determined successfully by using PSI displacement measurements (Notti et al. 2014).

In this study, C-Bant SAR SLC images belonging to Sentinel images are exploited. Considering the aim of the project, SAR images with high spatial and spectral properties can be chosen by the user. Moreover, different band lengths e.g. L, X or P can be employed according to the scattering properties on the topography e.g. vegetation density, slope. Hence, number of PS points, density of the measurement in time series and the accuracy of the displacements will be higher.

PSInSAR method is useful to be employed to determine the borders of the landslide in the cases where it is not determined technically because of safety, health or accessibility reasons. But, the mechanisms of landslide like sliding surface and sliding depth, slope stability and landslide mass cannot be identified by PSInSAR technique, instead a detailed geological and geo-technical investigations need to be carried out in the area. PSInSAR is an efficient technique by itself to identify the displacement in LOS direction, but according to the aim of the project (e.g. modelling landslide) where the PSInSAR is not sufficient alone, it can be used as supplementary data or to validate the final product. Finally, it can be concluded that working in large areas with this method will be cost-effective and will last shorter compared to the traditional terrestrial methods.

6. Conclusions

In this study, landslide areas in Havuzlu village belonging to Yusufeli province in Artvin city in northeast side of Turkey are monitored and determined by PSInSAR method using Sentinel 1A SAR images.

In total, 24 C Band images with VV polarization in ascending orbit are downloaded and their acquisition time is around the same time with the measurement period of reference points. At the end of this study, total displacement in Havuzlu is found between −25 and +28 mm/year by using PSInSAR method.

In total, 1608 PS points are generated by PSInSAR technique. Generally, PS points appear in rocky areas and in the city centres as these areas include most of the persistent scattering objects compared to the landslide areas. In this study, the velocity of points in the landslide area is found higher than the rest of the PS points in the study area. That

indication helped us to identify the unstable areas from other areas. The validation of the PSInSAR method is carried out in two ways. In the first way, when the reference points (DEF-2 and DEF-13) and PS points around them are compared to each other, we found that the direction of their displacements and their trends are the same. 1D displacements of DEF-2 and the nearest PS point around it, which is ∼9.8 m away, are −0.43 mm/year and −2.77 mm/year, respectively. The mean displacement of five PS points around DEF-2 is −5.21 mm/year. In the case of the reference point DEF-13 and the nearest PS point around it which is ∼15.2 m away are −1.84 mm/year and −14.96 mm/year, respectively. The mean displacement of eight PS points around DEF-13 is −6.65 mm/year. The difference between the reference point's displacement and the mean displacements PS points are below 1 cm in line of sight direction and as their signs are negative, both displacements are subsidence in the landslide area. In addition to this comparison, the reference point's (DEF-2 and DEF-13) 1D displacements obtained from field measurements are presented in a time series graphic together with the displacement of PS points around it. It can be seen from the graphics that the displacements of PS points obtained by PSInSAR technique are similar to the displacements of the reference points. In the second way, where both old and new displacement values of the reference points are compared to each other, it is seen that the maximum and minimum differences which are below 3 mm were obtained at DEF-2 as +3.02 mm/year and at DEF-5 as +0.10 mm/year, respectively. Moreover, having the signs of the new displacements values the same for both displacements show that the values calculated by PSInSAR method are consistent with the reference points. After two different validation processes, it is showed that the displacements found by PSInSAR method are consistent with the reference point's displacements measured in the study area. PSInSAR is an useful method to monitor the displacement in large fields in short time. In the context of dam safety, monitoring dam reservoir over time contributes relevant information on their future behaviour and helps authorities to give decisions accordingly.

ORCID

Bulent Volkan Yazici http://orcid.org/0000-0001-7847-2735
Esra Tunc Gormus http://orcid.org/0000-0002-3334-2061

References

Arikan M, Hanssen RF. 2008. Structral deformation of the high speed line HSL infrastructure in the Netherlands; observations using satellite radar interferometry In 13th FIG International Symposium on Deformation Measurements and Analysis, Lisbon, Portugal. p. 12–15.

Arnaud A, Adam N, Hanssen R, Inglada J, Duro J, Closa J, Eineder M. 2003. Asar ers interferometric phase continuity. Paper presented at the IGARSS 2003. IEEE International Geoscience and Remote Sensing Symposium, Toulouse, France. Vol. 2, p. 1133–1135.

Arun P. 2013. A comparative analysis of different dem interpolation methods. Egypt J Remote Sens Space Sci. 16(2):133–139.

Bayer B, Simoni A, Mulas M, Corsini A, Schmidt D. 2018. Deformation responses of slow moving landslides to seasonal rainfall in the northern Apennines, measured by InSAR. Geomorphology. 308: 293–306.

Casagli N, Cigna F, Bianchini S, Hölbling D, Füreder P, Righini G, Del Conte S, Friedl B, Schneiderbauer S, Iasio C, et al. 2016. Landslide mapping and monitoring by using radar and optical remote sensing: examples from the ec-fp7 project safer. Remote Sens Appl: Soc Environ. 4:92–108.

Ciampalini A, Raspini F, Lagomarsino D, Catani F, Casagli N. 2016. Landslide susceptibility map refinement using psinsar data. Remote Sens Environ. 184:302–315.

Colesanti C, Ferretti A, Prati C, Rocca F. 2001. Comparing GPS, optical leveling and permanent scatterers. Paper presented at the IGRASS 2001. Scanning the Present and Resolving the Future. Proceedings of

IEEE 2001 International Geoscience and Remote Sensing Symposium, Sydney, Australia, Vol. 6, p. 2622–2624.
Comut FC. 2016. Farklı yeryüzü Özelliklerinde İleri insar teknikleri kullanılarak yüzey deformasyonlarının belirlenmesi, doktora tezi [Unpublished doctoral dissertation]. Kenya: Selçuk Üniversitesi, Fen Bilimleri Enstitüsü.
Copernicus. 2018. Copernicus open access hub; [accessed 20 June 2018]. https://scihub.copernicus.eu/dhus/.
Costantini M, Iodice A, Magnapane L, Pietranera L. 2000. Monitoring terrain movements by means of sparse SAR differential interferometric measurements. Paper presented at the IEEE 2000 International Geoscience and Remote Sensing Symposium, Honolulu, USA, Vol. 7, p. 3225–3227.
Farina P, Colombo D, Fumagalli A, Marks F, Moretti S. 2006. Permanent scatterers for landslide investigations: outcomes from the esa-slam project. Eng Geol. 88(3–4):200–217.
Ferretti A, Prati C, Rocca F. 2001. Permanent scatterers in sar interferometry. IEEE Trans Geosci Remote Sens. 39(1):8–20.
Ferretti A, Savio G, Barzaghi R, Borghi A, Musazzi S, Novali F, Prati C, Rocca F. 2007. Submillimeter accuracy of insar time series: experimental validation. IEEE Trans Geosci Remote Sens. 45(5): 1142–1153.
Gabriel AK, Goldstein RM, Zebker HA. 1989. Mapping small elevation changes over large areas: differential radar interferometry. J Geophys Res. 94(B7):9183–9191.
Hooper A, Bekaert D, Hussain E, Spaans K. 2010. StaMPS/MTI manual. Delft Institute of Earth Observation and Space Systems Delft University of Technology, Kluyverweg, 1, 2629.
Hooper A, Bekaert D, Spaans K, Ar Ikan M. 2012. Recent advances in sar interferometry time series analysis for measuring crustal deformation. Tectonophysics. 514–517:1–13.
Hooper A, Zebker H, Segall P, Kampes B. 2004. A new method for measuring deformation on volcanoes and other natural terrains using insar persistent scatterers. Geophys Res Lett. 31(23).
Kampes BM. 2006. Radar interferometry persistent scatterer technique. Dordrecht, The Netherlands: Springer.
Köthur P, Eggert D, Schenk A, Sips M. 2016. Visual analytics for persistent scatterer interferometry: first steps and future challenges. In Andrienko N, Sedlmair, M, editors. Eurovis workshop on visual analytics (Eurova). The Eurographics Association; p. 37–41.
Lagios E, Sakkas V, Novali F, Bellotti F, Ferretti A, Vlachou K, Dietrich V. 2013. Squeesar™ and gps ground deformation monitoring of santorini volcano (1992–2012): tectonic implications. Tectonophysics. 594:38–59.
Massonnet D, Feigl KL. 1998. Radar interferometry and its application to changes in the earth's surface. Rev Geophys. 36(4):441–500.
Mateos RM, Ezquerro P, Luque-Espinar JA, Béjar-Pizarro M, Notti D, Azañón JM, Montserrat O, Herrera G, Fernández-Chacón F, Peinado T, et al. 2017. Multiband psinsar and long-period monitoring of land subsidence in a strategic detrital aquifer (Vega de Granada, se Spain): an approach to support management decisions. J Hydrol. 553:71–87.
Meisina C, Zucca F, Fossati D, Ceriani M, Allievi J. 2006. Ground deformation monitoring by using the permanent scatterers technique: the example of the Oltrepo Pavese (Lombardia, Italy). Eng Geol. 88(3–4):240–259.
Notti D, Herrera G, Bianchini S, Meisina C, García-Davalillo JC, Zucca F. 2014. A methodology for improving landslide PSI data analysis. Int J Remote Sens. 35(6):2186–2214.
Scaioni M, Longoni L, Melillo V, Papini M. 2014. Remote sensing for landslide investigations: an overview of recent achievements and perspectives. Remote Sens. 6(10):9600–9652.
Singhroy V, Mattar K, Gray A. 1998. Landslide characterisation in Canada using interferometric SAR and combined SAR and TM images. Adv Space Res. 21(3):465–476. (Remote Sensing: Inversion Problems and Natural Hazards)
Tamburini A, Bianchi M, Giannico C, Novali F. 2010. Retrieving surface deformation by psinsar™ technology: a powerful tool in reservoir monitoring. Int J Greenhouse Gas Control. 4(6):928–937.
Tofani V, Raspini F, Catani F, Casagli N. 2013. Persistent scatterer interferometry (PSI) technique for landslide characterization and monitoring. Remote Sens. 5(3):1045–1065.
Tural S. 2011. Gerçek zamanlı meteoroloji verilerinin toplanması, analizi ve haritalanması, yüksek lisans tezi [Unpublished doctoral dissertation]. Ankara: Ankara Üniversitesi, Fen Bilimleri Enstitüsü.
Vertex. 2018. Alaska satellite facility's data portal; [accessed 25 June 2018]. https://vertex.daac.asf.alaska.edu/.
Vilardo G, Ventura G, Terranova C, Matano F, Nardò S. 2009. Ground deformation due to tectonic, hydrothermal, gravity, hydrogeological, and anthropic processes in the Campania region (Southern

Italy) from permanent scatterers synthetic aperture radar interferometry. Remote Sens Environ. 113(1): 197–212.
Wasowski J, Bovenga F. 2014. Investigating landslides and unstable slopes with satellite multi temporal interferometry: current issues and future perspectives. Eng Geol. 174:103–138.
Yaprak S, Arslan E. 2008. Kriging yöntemi ve geoit yüksekliklerinin enterpolasyonu. Jeodezi, Jeoinformasyon ve Arazi Yönetimi Dergisi. 98:36–42.
Zebker HA, Goldstein RM. 1986. Topographic mapping from interferometric synthetic aperture radar observations. J Geophys Res. 91(B5):4993.
Zhang L, Lu Z, Ding X, Jung H, Feng G, Lee C-W. 2012. Mapping ground surface deformation using temporarily coherent point sar interferometry: application to los angeles basin. Remote Sens Environ. 117:429–439.